Scripta Materialia 153 (2018) 90–93

Contents lists available at ScienceDirect

Scripta Materialia

journal homepage: www.elsevier.com/locate/scriptamat

Regular article

Larger strain recovery characteristics of Ti-Ni-Hf shape memory alloy composite under compression

Xiaoyang Yi, Xianglong Meng *, Wei Cai, Liancheng Zhao

School of Materials Science and Engineering, Harbin Institute of Technology, Harbin 150001, China

ARTICLE INFO

Article history:
Received 23 March 2018
Received in revised form 25 April 2018
Accepted 4 May 2018
Available online xxxx

Keywords:
Ti-Ni-Hf shape memory alloy
Superelasticity
Network structure
H precipitate
Composite

ABSTRACT

The quasi-continuous network microstructure was constructed by the in-situ HfC particles and TiB whiskers in the Ti-Ni-Hf alloy composite. Meanwhile, the fine and coherent H phase precipitated owing to the depletion of Ti and Hf in the matrix. Both the H precipitates and the quasi-continuous network microstructure jointly enhanced the matrix strength, and had no severe constraint or obstruction on the accommodation of transformation strain or stress during stress-induced martensitic transformation. Thus, the superior superelasticity with the recoverable strain of 9.5% can be obtained in the present Ti-Ni-Hf composite, which further widened their application fields.

© 2018 Acta Materialia Inc. Published by Elsevier Ltd. All rights reserved.

Ti-Ni-Hf alloys are the most potential high temperature shape memory alloy due to the higher transformation temperatures, excellent actuation fatigue, larger work outputs, superior damping capacity and two-way shape memory effect [1–4]. Moreover, the ternary Hf addition not only can improve the critical stress for the stress-induced martensite transformation, but also increase the theoretical transformation strains [5].

In practice, the polycrystalline Ti-Ni-Hf alloys show less recoverable strains derived from the shape memory effect (SME). In addition, the simultaneous occurrence of stress induced martensite and dislocation slip results in the absence of the superelasticity (SE) [1,6,7]. Several measures including the solution strengthening, precipitation strengthening, the fabrication of the single crystal and/or the combination of the above mentioned methods can strengthen the matrix and further achieve the superior superelasticity in Ti-Ni-Hf alloys [6–15]. Besides, the effect of the aging and the crystal orientation on the superelasticity behaviors as well as the tension-compression asymmetry of superelasticity behavior in Ti-Ni-Hf alloys also has been investigated systematically [15–17]. So far, the excellent superelasticity with maximum recoverable strain is 4% in an aged Ni-rich polycrystalline Ti50.3-Ni29.7-Hf20 (at.%) alloy under compression, while the largest local compressive superelasticity with 6.01% recoverable strain can be obtained in the aged Ni-rich Ti50.6-Ni24.4-Hf25 (at.%) polycrystalline alloy [18,19]. The perfect superelasticity with the compressive recoverable strain is 6% in the solution treated [111]-oriented Ni-Ti-Hf-Pd single crystal [20]. Nevertheless, compared with the maximum recoverable strain of 10% in binary Ti-Ni alloys and the theoretical compressive transformation strain of 9.5% in single crystalline Ti-Ni-Hf alloys, the characteristics of the lower recoverable strain for the polycrystalline Ti-Ni-Hf based alloys still restrict their extensive applications [21]. Recently, it has been reported that a quasi-continuous network structure is introduced into the Ti-based composite by the in-situ reaction, which not only enhances the matrix strength, but also maintains the moderate ductility on the basis of the connectivity of matrix [22]. Thus, the quasi-continuous network structure is designed in the Ti-Ni-Hf alloy composite by in-situ reaction hot pressed sintering in the present study. And it is expected that such a network structure is in favor of enhancing the matrix strength simultaneously without severely constraining the stress induced martensite transformation and obtaining the superior superelasticity.

In the present study, the spherical Ti36-Ni49-Hf15 (at.%) alloy powders with particle sizes ranging from 45 μm to 75 μm and B_4C particles with about 5 μm in size were chosen to fabricate the Ti-Ni-Hf alloy composite, which was in favor of good compactness and properties [23]. The Ti-Ni-Hf alloy powders were fabricated by plasma rotating electrode process (PREP) and the B_4C powders were purchased from the Trillion Metals Co., Ltd. The detailed procedures were shown in Fig. 1. Firstly, the mixtures of 100 g Ti-Ni-Hf alloy powders and 1 g B_4C particles were obtained by the low energy balling (200 r/min, 300 min, ball-to-powder ratio = 5:1) under high pure Ar atmosphere, making the B_4C particles uniformly attached the surface of Ti-Ni-Hf alloy powders. Secondly, the mixtures were poured into φ 25 mm graphite die and hot pressed sintered at 1100 °C for 60 min under higher vacuum (2×10^{-3} Pa). To ensure the compactness of the sample, the whole sintering process was maintained at 60 MPa pressure. The Ti-Ni-Hf alloy composite was synthesized via the hot pressed sintering (HPS).

---

* Corresponding author.
E-mail address: xlmeng@hit.edu.cn (X. Meng).

https://doi.org/10.1016/j.scriptamat.2018.05.006
1359-6462/© 2018 Acta Materialia Inc. Published by Elsevier Ltd. All rights reserved.

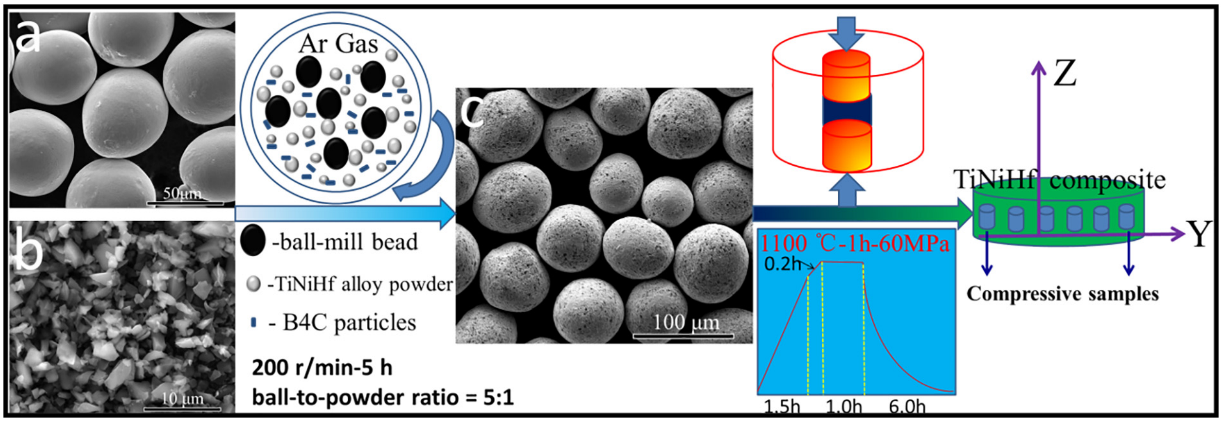

Fig. 1. Flow chart showing the processing route equipped with the SEM micrographs and schematic illustrations a: Ti-Ni-Hf alloy powders b: B_4C powders c: the blended mixture of Ti-Ni-Hf alloy powders and B_4C powders.

The subsequent testing samples were prepared from the Ti-Ni-Hf alloy composite by electric spark discharging machine.

The phase identification of Ti-Ni-Hf alloy composite was carried out by X-ray diffraction (XRD) with Cu K_α radiation at room temperature. The microstructural observations were performed on a scanning electron microscope (SEM) in a back-scattered electron model, and transmission electron microscope (TEM) with the operating voltage of 200 kV. The sample for TEM observations was prepared by ion beam thinning. The mechanical properties were obtained by an Instron-5569 testing system equipped with a thermal chamber. The cylinders having a size of φ 3 mm × 5 mm were used to characterize the superelastic responses. In order to investigate the superelastic responses of the Ti-Ni-Hf alloy composite, the sample was deformed at near or above A_f ($A_f = 49.5$ °C) under the compressive strain control and then unloaded under compressive force control. In the initial cycle, the sample was compressed to 4% strain and then unloaded. In the following cycles, the applied strain was increased by 2% and the maximum applied strain was 10%. In addition, the Ti-Ni-Hf alloy composites were tested under the successively incremental strain at various temperatures to investigate the dependence of the temperature on the transformation stress levels. All mechanical tests were performed at a strain rate of 0.2 mm/min.

Fig. 2a shows the back-scattered SEM images of the sintered Ti-Ni-Hf alloy composite. The microstructure of the present Ti-Ni-Hf alloy composite is characterized by the some black and white particles dispersed into the grey matrix. The second phase particles exhibit regular distribution. Among, a large proportion of white second phase particles closely connect, while the black second phase particles randomly distribute at the nearby of the white second phase particles. Both of them jointly construct a network structure. The size of the network structure is about 50 μm, which is similar to that of the original Ti-Ni-Hf alloy powder. It indicates that the second phase particles mainly form at the surface of the original Ti-Ni-Hf alloy powders. Besides, some white particles with several microns in size are observed in the interior of the network structure, which may be related to the difference in the diffusion rates. In order to determine the chemical composition of the second phase particles, an energy-dispersive spectroscopy (EDS) line scan across the second phase particles is performed. From the Fig. 2b, it is obvious that the contents of Hf and C are higher in the white particles, while the black particles are richer in the contents of Ti and B. In addition, combined with the XRD results of the Ti-Ni-Hf alloy composite in Fig. 2c, it can be speculated that the white and black second phase particles are HfC and TiB phase, respectively. This indicates that the reaction between Ti-Ni-Hf alloy powders and B_4C particles during HPS can be expressed by the following chemical equation: $4Ti + Hf + B_4C \rightarrow 4TiB + HfC$, which is consistent with the lower Gibbs formation energy of HfC and TiB phase [24,25]. Both HfC particle and TiB whisker are featured with the higher hardness and strength, which are frequently used for reinforcement in the composite [24,25].

Fig. 2d–f represents the bright field TEM image, the selected area electron diffraction (SAED) pattern and the HRTEM image of the Ti-Ni-Hf alloy composite, respectively. A high density of fine precipitates with spindle-shape morphology homogeneously distributed in the matrix of the Ti-Ni-Hf alloy composite. Fig. 2e shows extra diffraction spots at 1/3 and 2/3 of the distances along the matrix spots that correspond to the precipitate. The precipitate has a face-centered orthorhombic lattice structure as named H phase in the reported Ni-rich Ti-Ni-Hf based alloys [26–30], according to the electron diffraction patterns in Fig. 2e, which is

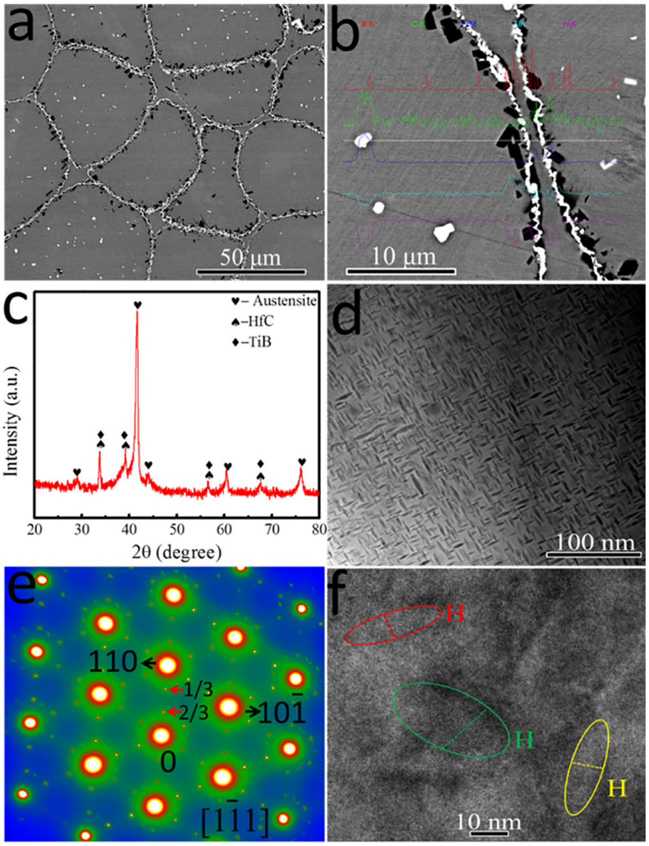

Fig. 2. The microstructure of Ti-Ni-Hf alloy composite a: The back-scattered SEM micrograph b: the results of EDS line scan c: The XRD pattern d: The bright field TEM image e: The corresponding SAED pattern f: The HRTEM images corresponding to the matrix and H precipitates with different orientation.

Download English Version:

https://daneshyari.com/en/article/7910605

Download Persian Version:

https://daneshyari.com/article/7910605

Daneshyari.com